Discrete time crystals with absolute stability

Krzysztof Giergiel[1,2], Jia Wang[3], Bryan J. Dalton[3], Peter Hannaford[2], and Krzysztof Sacha[1]

[1]*Instytut Fizyki Teoretycznej, Uniwersytet Jagielloński, ulica Profesora Stanislawa Lojasiewicza 11, PL-30-348 Kraków, Poland*
[2]*Optical Sciences Centre, Swinburne University of Technology, Melbourne 3122, Australia*
[3]*Centre for Quantum Technology Theory, Swinburne University of Technology, Melbourne 3122, Australia*

We show that interacting bosons on a ring which are driven periodically by a rotating potential can support discrete time crystals whose absolute stability can be proven. The absolute stability is demonstrated by an exact mapping of discrete-time-crystal states to low-lying eigenstates of a time-independent model that reveals spontaneous breaking of space translation symmetry. The mapping ensures that there are no residual time-dependent terms that could lead to heating of the system and destruction of discrete time crystals. We also analyze periodically kicked bosons where the mapping is approximate only and cannot guarantee the absolute stability of discrete time crystals. Besides illustrating potential sources of instability, the kicked bosons model demonstrates a rich field for investigating the interplay between different time and space symmetry breaking, as well as the stability of time crystal behavior in contact with a thermal reservoir.

Ordinary space crystals correspond to periodic distributions of particles in space which form despite the fact that the Hamiltonian is invariant under a translation of all the particles by an arbitrary vector. This is the phenomenon of spontaneous breaking of the continuous space translation symmetry into a discrete space translation symmetry in a time-independent many-body system. In 2012, research on time crystals was initiated where spontaneous breaking of time translation symmetry is responsible for the formation of a crystalline structure [1]. Periodically driven many-body closed systems can form discrete time crystals as a nonequilibrium quantum state in which the stable system response occurs at integer multiples of the drive period [2–5]. The discrete time translation symmetry of a time-periodic Hamiltonian is spontaneously broken and new periodic motion emerges—a novel crystalline structure appears in time [2].

The stability of discrete time crystals is much less obvious than for space crystals because the quasienergy spectrum of the Floquet Hamiltonian has no lower bound [6]. The key question arises as to whether discrete time crystals are really stable or they gradually absorb energy from the drive and eventually heat up to a structureless infinite temperature state, as expected for a generic periodically driven many-body system [7–9].

Systems which do not thermalize are typically integrable systems, but integrability is fragile and usually requires fine-tuning of system parameters [10–15]. Time-independent many-body systems in the presence of disorder are believed to reveal many-body localization (MBL) and emergent integrability [16–19]. Therefore, periodically driven MBL systems are potential candidates for realization of discrete time crystals [3,4,20]. However, the stability of discrete time crystals in driven MBL systems [21–24] is far from being obvious [25–32]—even in the time-independent case, the MBL is still debated [33,34]. Also, the stability of the first proposed discrete time crystal in ultracold bosonic atoms bouncing

resonantly on an oscillating atom mirror [2] has not been proven. While previous studies have demonstrated the stability of discrete time crystals for evolution times longer than those of realistic experiments [35–37], their validity in the context of an infinite number of bosons and infinite evolution time remains unproven.

Here, we show that resonantly driven bosons by a rotating potential on a ring in the Lieb-Liniger (LL) model can reveal discrete time crystals whose stability can be proven. Eigenstates of the Floquet Hamiltonian that break the discrete time translation symmetry can be mapped to low-energy eigenstates of a time-independent Hamiltonian in the rotating frame. The latter eigenstates are stable and reveal spontaneous breaking of *space* translation symmetry in the rotating frame, which corresponds to spontaneous breaking of the discrete *time* translation symmetry of the original model. This model concretely provides an example of the absence of quantum thermalization and the existence of stable time crystals in a closed quantum many-body system without the need for either disorder or integrability. Furthermore, an experimental realization of this model should be possible, since ultracold atoms on a ring have been created and applying a periodic drive potential should be straightforward [38–42].

Let us consider N bosons with contact interactions on a ring with circumference 2π which are periodically driven by a rotating potential

$$H = H_{\rm LL} + \sum_{i=1}^{N} V(2x_i - \omega t), \qquad (1)$$

$$H_{\rm LL} = \sum_{i=1}^{N} \frac{p_i^2}{2} + g_0 \sum_{i<j}^{N} \delta(x_i - x_j), \qquad (2)$$

where we use R and $\hbar^2/mR^2$ for the length and energy units, respectively, where R is the ring radius and m the mass of the bosons, and g_0 stands for the strength of the contact

interactions [43]. We assume that the potential in (1) has a double-well structure which remains unchanged if $x_i \to x_i + \pi$. Apart from such a discrete space translation symmetry, the Hamiltonian possesses also a discrete time translation symmetry, i.e., $t \to t + T$ (where $T = 2\pi/\omega$). We will see that for sufficiently strong interactions, these symmetries can spontaneously be broken and the system starts evolving with a period of $2T$ forming a discrete time crystal.

Let us investigate the system in the moving frame of the rotating potential, where we first perform a time-dependent unitary transformation $U_t = \exp(i \sum_j p_j \omega t/2)$, leading to a shift in the positions, $x_i \to x_i + \omega t/2$, and next a second time-independent unitary transformation $U_p = \exp(-i \sum_j x_j \omega/2)$, leading to a shift in the momenta, $p_i \to p_i + \omega/2$ [44]. Under these transformations, we end up with the following exact time-independent Hamiltonian:

$$\tilde{H} = \sum_{i=1}^{N} \left[\frac{p_i^2}{2} + V(2x_i) \right] + g_0 \sum_{i<j}^{N} \delta(x_i - x_j), \qquad (3)$$

where a constant term has been omitted. The state vector in the moving frame is related to that in the laboratory frame via $\tilde{\psi} = U_p U_t \psi$ [38].

Suppose that the discrete space translation symmetry of the Hamiltonian (3), i.e., the invariance under the shift $x_i \to x_i + \pi$, is spontaneously broken in the ground state and low-energy eigenstates, and only the symmetry related to the periodic boundary conditions on a ring remains. The corresponding time-independent single-particle probability densities in the moving frame, $\tilde{P}(x) = \int dx_2 \ldots dx_N |\tilde{\psi}(x, x_2, \ldots, x_N)|^2$, fulfill the periodic boundary conditions, $\tilde{P}(x + 2\pi) = \tilde{P}(x)$, but $\tilde{P}(x + \pi) \neq \tilde{P}(x)$. When we return to the original laboratory frame by means of the inverse U_p and U_t transformations, the laboratory probability densities read $P(x, t) = \tilde{P}(x - \omega t/2)$ [38], and thus, due to the spontaneous breaking of the space translation symmetry of the Hamiltonian (3), they now also reveal spontaneous breaking of the discrete time translation symmetry of the Hamiltonian (1), since $P(x, t)$ is periodic with the period $2T$ but not with the period T. Hence, the system spontaneously starts evolving with a period which is an integer multiple of the period dictated by the drive and forms a discrete time crystal.

Spontaneous breaking of the space translation symmetry of the Hamiltonian (3) occurs in the thermodynamic limit (i.e., for $N \to \infty$, $g_0 \to 0$ but $g_0 N = \text{const}$, and the circumference of the ring is always equal to 2π). In this limit the ground state of (3) is a Bose-Einstein condensate (BEC) where all bosons occupy the same single-particle wave function $\phi_0(x)$, which is the solution of the mean-field Gross-Pitaevskii equation [45]. If V is a symmetric double-well potential, then for sufficiently strong attractive interactions (i.e., for sufficiently negative $g_0 N$) there are two degenerate ground-state solutions $\phi_0(x)$ where one is localized around one potential minimum and the other around the second minimum, i.e., the self-trapping phenomenon is observed. This has been rigorously proven for the double-well potential in the form of Dirac-delta wells, $V \propto -\delta(x) - \delta(x + \pi)$ [46], and also demonstrated experimentally and theoretically in many different double-well potentials, e.g., see analytical solutions in [47]. The proof of the self-trapping phenomenon implies proof of the absolute

stability of the corresponding discrete time crystals, as the mapping is mathematically exact. In the following, instead of illustrating the formation of the discrete time crystals in the rotating Dirac-delta wells, we consider an example that can readily be realized in the laboratory [38], i.e., when $V = \lambda \cos(2x)$. For sufficiently negative $g_0 N$, the ground state reveals the self-trapping phenomenon, where we illustrate the spontaneous symmetry breaking in detail.

In the presence of the external potential ($\lambda \neq 0$) and when the attractive interaction is very small, and in the thermodynamic limit, the ground state of the system (3) is a BEC where all bosons occupy the single-particle ground state $\phi_0(x)$, which is a balanced superposition of two wave packets localized in each well of the external potential in (3) [45]. The width of the wave packets can be estimated by employing the harmonic oscillator approximation for the potential wells and it reads $\sigma \approx 1/\sqrt{\Omega}$, where the frequency of the harmonic oscillator $\Omega = 2\sqrt{\lambda}$. In the presence of the attractive interactions ($g_0 < 0$) and increasing their strength, we enter a self-trapping regime for bosons where the mean-field lowest-energy solutions are degenerate and each of them can be approximated by all bosons occupying a single wave packet localized in one well of the external potential [45,46]. The space translation symmetry of the Hamiltonian (3) is spontaneously broken, and the self-trapped states live forever in the thermodynamic limit. Increasing further the strength of the attractive interactions, we enter the bright soliton regime [45], i.e., the wave packets localized in the potential wells start shrinking due to strong attractive interactions and resembling the bright soliton solutions. Thus we can observe three regimes: (i) a weakly interacting regime with no spontaneous symmetry breaking, (ii) a moderate-interaction regime and spontaneous breaking of the space translation symmetry of (3), and (iii) a strong-interaction regime, where the spontaneous breaking of the symmetry corresponds to the formation of bright soliton wave packets of width $\xi = 2/|g_0(N-1)| < \sigma$, the width of the single-particle ground state in the potential well [45].

In order to diagonalize the Hamiltonian (3), we employ the eigenbasis of the undriven Lieb-Liniger model, which can be obtained with the help of the Bethe ansatz [38,48,49]. Diagonalization of the Hamiltonian matrix yields the energy spectrum of (3), depicted in Fig. 1 as a function of $g_0(N-1)$ for $N = 9$ and $\lambda = 1.5$. Let us first focus on the strongest interactions presented in Fig. 1(a), which are in the regime (iii), where the width ξ of the bright soliton becomes smaller than the width σ of the single-particle ground state in the potential well, i.e., when $|g_0(N-1)| \gtrsim 2\sqrt{2}\lambda^{1/4} = 3.13$ for $\lambda = 1.5$. Without the external potential ($\lambda = 0$), the lowest-energy solution within the mean-field approach would represent a bright soliton, $\phi_0(x - q) = \cosh^{-1}[(x - q)/\xi]/\sqrt{2\xi}$, which is occupied by all bosons and can be localized at any point q on the ring [50]. In the presence of the double-well potential ($\lambda \neq 0$) and for $\xi < \sigma$, there are two possible ground-state locations of the soliton at the bottoms of the potential wells, i.e., $q = \pi/2$ or $3\pi/2$. Low-energy excitations of the bright soliton correspond to excitations of its center of mass, depicted by the green lines in Fig. 1(a) [38]. When we decrease the strength of the attractive interactions, we lose such a *single-body* character of the low-energy
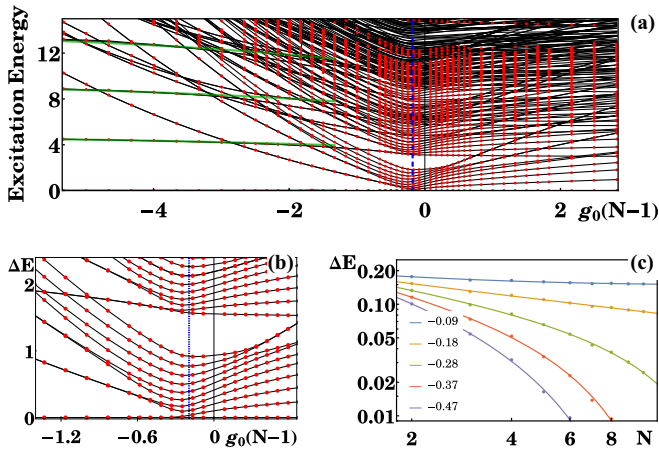
FIG. 1. (a) Solid black lines show the excitation spectrum of (3), i.e., eigenenergies minus the ground-state energy, for $N = 9$ and $\lambda = 1.5$. Vertical dashed line indicates the critical value of $g_0(N - 1)$ for the quantum phase transition to the discrete-time-crystal regime obtained for $N \to \infty$ from the results presented in (c). Green lines are related to the ground-state level and excited levels of the center of mass of the system [38], which are doubly degenerate because the bosons can be located in one of the wells of the double-well potential. Red circles are exact quasienergies of the kicked LL model (cf. (4) with $T = \pi/31$ [44]) that are relevant to time crystal states and which are perfectly reproduced by the spectrum of (3). (b) An enlargement of (a) in the vicinity of the critical point. (c) Log-log plots of the difference, ΔE, between the lowest eigenenergies of (3) vs N for different fixed values of $g_0(N - 1)$, as indicated in the figure. The critical value of $g_0(N - 1) \approx -0.18$ corresponds to an algebraic decrease of ΔE with N, and this agrees with the two-mode prediction for $N \to \infty$ [38]. For weaker interactions ΔE approaches a constant value, while for stronger interactions, ΔE decreases exponentially with N.
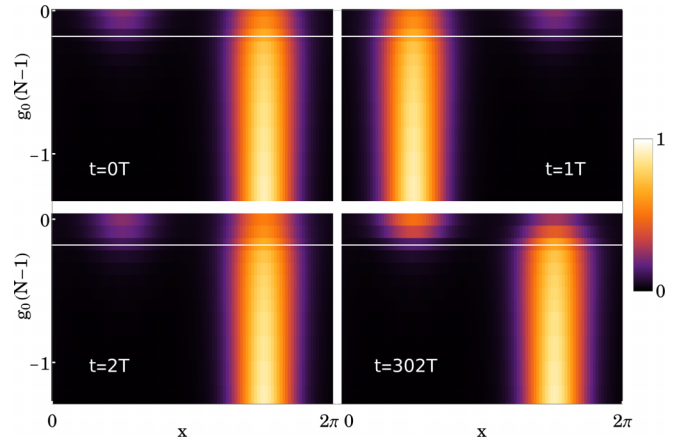

FIG. 2. Single-particle probability densities corresponding to superpositions of the two lowest-energy eigenstates of (3) plotted in the laboratory frame for different moments of time as indicated in the panels for $N = 9$. In each panel, collections of the densities for different interaction strengths $g_0(N - 1)$ are presented. Solid white lines indicate the critical interaction strength $g_0(N - 1) \approx -0.18$ for the transition to the discrete-time-crystal regime when $N \to \infty$. Densities above these lines reveal a decay of the $2T$-periodic evolution due to tunneling—for noninteracting bosons, complete tunneling takes place at $t \approx 302T$. Densities below the solid white lines show discrete-time-crystal evolution for $N \to \infty$. The other parameters are the same as in Fig. 1, i.e., $\lambda = 1.5$ and $T = \pi/31$ [44].

spectrum which takes place for $\xi \gtrsim \sigma$. Then low-energy excitations lead to quantum depletion of a BEC localized in one of the potential wells and transfer of bosons to the other well [51–53]. This moderate-interaction regime corresponds to the self-trapping of a BEC where bosons prefer to localize in one of the potential wells but do not form a bound state like in the bright soliton case. The self-trapping properties are observed in the ground and excited eigenstates up to the so-called symmetry-breaking edge, i.e., the corresponding excitation energy is proportional to N, and the number of states that break the symmetry is extensive, which is crucial in order to call discrete time crystals a new phase [38].

One can ask how weak the attractive interactions should be in order to recover the space translation symmetry of (3). The critical interaction strength for the phase transition between the symmetry-broken and symmetry-preserving phases can be estimated by means of the two-mode approach, because the interactions in this regime are weak and not able to modify the shape of the single-particle wave packets localized in the potential wells which are used in the two-mode approximation [2,38,51]. Indeed, the two-mode prediction agrees with the numerical results shown in Fig. 1(c), where at the critical value of $g_0(N - 1) \approx -0.18$, the energy gap between the lowest-energy eigenstates decreases algebraically with N. For stronger interactions the gap decreases exponentially, while

for weaker interactions it approaches a constant value [2]. Thus if the interactions are sufficiently strong and $N \to \infty$, the symmetry-preserving eigenstates are degenerate and their superpositions form symmetry-broken eigenstates which live forever.

When we return to the laboratory frame, the symmetry-broken eigenstates of (3) will evolve with a period of $2T$, demonstrating discrete time crystals with absolute stability. In Fig. 2 we present the time evolution of superpositions of the lowest symmetry-preserving eigenstates of (3) for different interaction strengths. At $g_0(N - 1) \approx -0.18$ and for $N \to \infty$, the quantum phase transition to the discrete-time-crystal regime occurs where the superpositions evolve with the period $2T$—for $N = 9$ the ground-state level becomes practically degenerate for stronger interactions, i.e., $g_0(N - 1) \approx -0.3$. At slightly stronger interactions, excited levels also become practically doubly degenerate, indicating that with increasing N there is an extensive number of states that reveal time crystal behavior. At $g_0(N - 1)$ around -3, there is a crossover to the bright soliton regime where low-energy excitations have *single-body* character, because bosons form a bound bright soliton state [54–56].

It is important to emphasize that the spontaneous emergence of the time crystal and its evolution with the period $2T$ is not a trivial observation of a time-independent problem in a rotating frame. If the interactions were too weak to induce spontaneous symmetry breaking, when returning from the rotating frame to the laboratory frame we would observe periodic evolution with the period T because such a period corresponds to the time translational symmetry of the Hamiltonian (1). Only when the interactions lead to symmetry

breaking do we observe the emergence of the time crystal and its evolution with the period $2T$.

Having analyzed the system (1), we will now switch to a system with a periodically kicked potential, which can also be experimentally implemented and has recently garnered significant interest [57,58]. Although the stability of discrete time crystals in the kicked LL model remains an open question, this model exhibits a range of different time and space symmetry breaking. Additionally, it provides intriguing opportunities to investigate the impact of a reservoir of a rotating thermal cloud on the stability of phases with broken symmetries. Let us exchange the time-periodic perturbation in the Hamiltonian (1) with

$$H_1 = \lambda T \sum_{i=1}^{N} \cos(2x_i) \sum_{m=-\infty}^{+\infty} \delta(t - mT), \qquad (4)$$

which describes periodic kicking of the particles with the period $T = 2\pi/\omega$. When we perform the same unitary transformation to the moving frame as previously, i.e., U_t, and a similar shift of the momenta U_p, then using the rotating-wave approximation or the Magnus expansion we can obtain an effective Hamiltonian identical to (3), see [38,59].

We have already analyzed the system (3); thus, in the present case of the time-periodic kicking (4), we have to demonstrate only that the low-energy eigenstates of (3) reproduce well the relevant exact eigenstates of the Floquet Hamiltonian, which are also eigenstates of the Floquet evolution operator. The Floquet evolution operator is the evolution operator of the system over a single driving period, which in the case of the time-periodic kicking (4) reads

$$U(T) = e^{-iH_{\mathrm{LL}}T} \, e^{-i\lambda T \sum_{i=1}^{N} \cos(2x_i)}. \qquad (5)$$

This unitary operator can be diagonalized in the eigenbasis of the LL Hamiltonian, and knowing its eigenphases ϕ_n, we can calculate the quasienergies of the system, $E_n = -\phi_n/T$. The obtained exact quasienergies, which are relevant to discrete-time-crystal states, are also shown in Fig. 1, and they are perfectly reproduced by the low-lying spectrum of (3). We have chosen the same λ as previously, and consequently, we expect exactly the same spectrum as in the case of the Hamiltonian (1); indeed, the obtained quasienergies are indistinguishable in the plot.

Both the system (1) and the kicked LL model (4) can be described using the Floquet formalism, where all physically relevant quasienergies lie in a single Floquet zone. For small values of N, Floquet states can be obtained numerically. However, very-high-order terms, which are neglected in numerical calculations, may introduce tiny couplings between Floquet states with similar quasienergies that can lead to the decay of discrete time crystals as $t \to \infty$, especially when we first take the $N \to \infty$ limit. In the case of the system (1), we know that quasienergies corresponding to the discrete time crystal can be unfolded and they correspond to the low-energy spectrum of the time-independent Hamiltonian (3). Furthermore, we have a guarantee that they are not coupled to any other Floquet states in any order. In the case of the kicked LL model, such absolute stability of the discrete time crystals cannot be guaranteed. The discrete time crystal in (1) has been designed so that the perturbation contains only one harmonic responsible for the formation of the crystal. In the case of the kicked LL model, there are many other harmonics whose influence can be reduced but cannot be fully eliminated.

So far we have analyzed the Floquet states that break both discrete space and time translational symmetry in the periodically kicked LL model by switching to the frame moving with the frequency $\omega/2$ by means of the unitary transformation U_t. Let us show that the periodically kicked LL model (4) can also support states that spontaneously break the discrete space translation symmetry without breaking the discrete time translation symmetry, which does not exist in the corresponding LL model driven by the rotating potential. To investigate these states, we can also switch to the moving frame but with the frequency ω, and we still obtain the same effective Hamiltonian (3) [38]. Then, however, eigenstates of (3) that reveal spontaneous breaking of the discrete space translation symmetry do not break the discrete time translation symmetry. Indeed, when we return to the laboratory frame, all eigenstates of (3) evolve with the driving period T.

The periodically kicked LL model is also attractive in studying the time crystal behavior in contact with a thermal bath. In the case of a rotating potential (1), the discrete time crystals should be accessible as a thermal equilibrium state in contact with a reservoir of rotating thermal atoms. In the case of (4), the situation becomes more intriguing, as in the rotating frame, the time-independent Hamiltonian (3) is only an approximation. Cooling of atoms in the presence of a rotating thermal cloud has been realized in experiments demonstrating vortices in a BEC [45]. So new opportunities for theoretical and experimental investigations of the stability of discrete time crystals in contact with a thermal reservoir are opening up.

To summarize, we have analyzed interacting bosons on a ring with various periodic perturbations, which turns out to be a suitable system for realization of discrete time crystals. Most importantly, for the case of a rotating potential [see (1)], this system can reveal discrete time crystals whose stability can be proven by an exact mapping of the discrete-time-crystal states to low-lying eigenstates of a time-independent Hamiltonian. The periodically driven bosons on a ring can also reveal big discrete time crystals and condensed matter in time [60–65]. For example, if we choose $\cos(sx_i - \omega t)$ as the potential in (1), then spontaneously emerging discrete time crystals can evolve with a period s times longer than the driving period, where $s \gg 1$.

[1] F. Wilczek, Phys. Rev. Lett. **109**, 160401 (2012).

[2] K. Sacha, Phys. Rev. A **91**, 033617 (2015).

[3] V. Khemani, A. Lazarides, R. Moessner, and S. L. Sondhi, Phys. Rev. Lett. **116**, 250401 (2016).

[4] D. V. Else, B. Bauer, and C. Nayak, Phys. Rev. Lett. **117**, 090402 (2016).

[5] N. Y. Yao, A. C. Potter, I.-D. Potirniche, and A. Vishwanath, Phys. Rev. Lett. **118**, 030401 (2017).

[6] K. Sacha, *Time Crystals* (Springer International Publishing, Switzerland, Cham, 2020).

[7] L. D'Alessio and M. Rigol, Phys. Rev. X **4**, 041048 (2014).

[8] A. Lazarides, A. Das, and R. Moessner, Phys. Rev. E **90**, 012110 (2014).

[9] P. Ponte, A. Chandran, Z. Papić, and D. A. Abanin, Ann. Phys. (Amsterdam) **353**, 196 (2015).

[10] M. Rigol, V. Dunjko, V. Yurovsky, and M. Olshanii, Phys. Rev. Lett. **98**, 050405 (2007).

[11] L. F. Santos and M. Rigol, Phys. Rev. E **81**, 036206 (2010).

[12] M. Rigol and L. F. Santos, Phys. Rev. A **82**, 011604(R) (2010).

[13] L. F. Santos and M. Rigol, Phys. Rev. E **82**, 031130 (2010).

[14] A. C. Cassidy, C. W. Clark, and M. Rigol, Phys. Rev. Lett. **106**, 140405 (2011).

[15] J.-S. Caux and F. H. L. Essler, Phys. Rev. Lett. **110**, 257203 (2013).

[16] R. Nandkishore and D. A. Huse, Annu. Rev. Condens. Matter Phys. **6**, 15 (2015).

[17] E. Altman and R. Vosk, Annu. Rev. Condens. Matter Phys. **6**, 383 (2015).

[18] L. D'Alessio, Y. Kafri, A. Polkovnikov, and M. Rigol, Adv. Phys. **65**, 239 (2016).

[19] M. Mierzejewski, M. Kozarzewski, and P. Prelovšek, Phys. Rev. B **97**, 064204 (2018).

[20] D. V. Else, B. Bauer, and C. Nayak, Phys. Rev. X **7**, 011026 (2017).

[21] P. Ponte, Z. Papić, F. M. C. Huveneers, and D. A. Abanin, Phys. Rev. Lett. **114**, 140401 (2015).

[22] A. Lazarides, A. Das, and R. Moessner, Phys. Rev. Lett. **115**, 030402 (2015).

[23] D. Abanin, W. D. Roeck, and F. Huveneers, Ann. Phys. **372**, 1 (2016).

[24] P. Sierant, M. Lewenstein, A. Scardicchio, and J. Zakrzewski, Phys. Rev. B **107**, 115132 (2023).

[25] J. Zhang, P. W. Hess, A. Kyprianidis, P. Becker, A. Lee, J. Smith, G. Pagano, I.-D. Potirniche, A. C. Potter, A. Vishwanath *et al.*, Nature (London) **543**, 217 (2017).

[26] S. Choi, J. Choi, R. Landig, G. Kucsko, H. Zhou, J. Isoya, F. Jelezko, S. Onoda, H. Sumiya, V. Khemani *et al.*, Nature (London) **543**, 221 (2017).

[27] S. Pal, N. Nishad, T. S. Mahesh, and G. J. Sreejith, Phys. Rev. Lett. **120**, 180602 (2018).

[28] J. Rovny, R. L. Blum, and S. E. Barrett, Phys. Rev. Lett. **120**, 180603 (2018).

[29] J. Smits, L. Liao, H. T. C. Stoof, and P. van der Straten, Phys. Rev. Lett. **121**, 185301 (2018).

[30] X. Mi, M. Ippoliti, C. Quintana, A. Greene, Z. Chen, J. Gross, F. Arute, K. Arya, J. Atalaya, R. Babbush *et al.*, Nature (London) **601**, 531 (2022).

[31] J. Randall, C. E. Bradley, F. V. van der Gronden, A. Galicia, M. H. Abobeih, M. Markham, D. J. Twitchen, F. Machado, N. Y. Yao, and T. H. Taminiau, Science **374**, 1474 (2021).

[32] P. Frey and S. Rachel, Sci. Adv. **8**, eabm7652 (2022).

[33] J. Z. Imbrie, J. Stat. Phys. **163**, 998 (2016).

[34] D. Sels and A. Polkovnikov, Phys. Rev. E **104**, 054105 (2021).

[35] J. Wang, P. Hannaford, and B. J. Dalton, New J. Phys. **23**, 063012 (2021).

[36] A. Kuroś, R. Mukherjee, W. Golletz, F. Sauvage, K. Giergiel, F. Mintert, and K. Sacha, New J. Phys. **22**, 095001 (2020).

[37] J. Wang, K. Sacha, P. Hannaford, and B. J. Dalton, Phys. Rev. A **104**, 053327 (2021).

[38] See Supplemental Material at http://link.aps.org/supplemental/10.1103/PhysRevB.108.L180201 for details of the description and analysis of Lieb-Liniger model driven by a rotating lattice potential and periodically kicked Lieb-Liniger model.

[39] S. Gupta, K. W. Murch, K. L. Moore, T. P. Purdy, and D. M. Stamper-Kurn, Phys. Rev. Lett. **95**, 143201 (2005).

[40] T. A. Bell, J. A. P. Glidden, L. Humbert, M. W. J. Bromley, S. A. Haine, M. J. Davis, T. W. Neely, M. A. Baker, and H. Rubinsztein-Dunlop, New J. Phys. **18**, 035003 (2016).

[41] S. Moulder, S. Beattie, R. P. Smith, N. Tammuz, and Z. Hadzibabic, Phys. Rev. A **86**, 013629 (2012).

[42] A. Kumar, N. Anderson, W. D. Phillips, S. Eckel, G. K. Campbell, and S. Stringari, New J. Phys. **18**, 025001 (2016).

[43] The interaction strength $g_0 = 2mR\omega_\perp a_s/\hbar$, where $\omega_\perp$ is the frequency of the harmonic transverse confinement and a_s is the atomic s-wave scattering length.

[44] Note that if $\omega/2$ is not an integer number, the original periodic boundary conditions become twisted boundary conditions after the transformation U_p, see [38]. For simplicity, we always choose integer values of $\omega/2$.

[45] C. Pethick and H. Smith, *Bose-Einstein Condensation in Dilute Gases* (Cambridge University Press, Cambridge, England, 2002).

[46] R. K. Jackson and M. I. Weinstein, J. Stat. Phys. **116**, 881 (2004).

[47] K. W. Mahmud, J. N. Kutz, and W. P. Reinhardt, Phys. Rev. A **66**, 063607 (2002).

[48] V. E. Korepin, N. M. Bogoliubov, and A. G. Izergin, *Quantum Inverse Scattering Method and Correlation Functions* (Cambridge University Press, Cambridge, UK, 1993).

[49] M. Gaudin, *The Bethe Wavefunction* (Cambridge University Press, Cambridge, England, 2014).

[50] Y. Castin, in *Coherent Atomic Matter Waves*, edited by R. Kaiser, C. Westbrook, and F. David (Springer Berlin Heidelberg, 2001), pp. 1–136.

[51] P. Ziń, J. Chwedeńczuk, B. Oleś, K. Sacha, and M. Trippenbach, EPL (Europhysics Letters) **83**, 64007 (2008).

[52] P. Ribeiro, J. Vidal, and R. Mosseri, Phys. Rev. E **78**, 021106 (2008).

[53] B. Oleś, P. Ziń, J. Chwedeńczuk, K. Sacha, and M. Trippenbach, Laser Phys. **20**, 671 (2010).

[54] J. Dziarmaga, Phys. Rev. A **70**, 063616 (2004).

[55] C. Weiss and Y. Castin, Phys. Rev. Lett. **102**, 010403 (2009).

[56] K. Sacha, C. A. Müller, D. Delande, and J. Zakrzewski, Phys. Rev. Lett. **103**, 210402 (2009).

[57] A. Cao, R. Sajjad, H. Mas, E. Q. Simmons, J. L. Tanlimco, E. Nolasco-Martinez, T. Shimasaki, H. E. Kondakci, V. Galitski, and D. M. Weld, Nat. Phys. **18**, 1302 (2022).

[58] J. H. See Toh, K. C. McCormick, X. Tang, Y. Su, X.-W. Luo, C. Zhang, and S. Gupta, Nat. Phys. **18**, 1297 (2022).

[59] S. Blanes, F. Casas, J. A. Oteo, and J. Ros, Eur. J. Phys. **31**, 907 (2010).

[60] K. Giergiel, A. Kosior, P. Hannaford, and K. Sacha, Phys. Rev. A **98**, 013613 (2018).

[61] K. Sacha, Sci. Rep. **5**, 10787 (2015).

[62] P. Hannaford and K. Sacha, AAPPS Bulletin **32**, 12 (2022).

[63] L. Guo, M. Marthaler, and G. Schön, Phys. Rev. Lett. **111**, 205303 (2013).

[64] L. Guo, *Phase Space Crystals*, 2053-2563 (IOP Publishing, Bristol, 2021).

[65] K. Giergiel, R. Lier, P. Surówka, and A. Kosior, Phys. Rev. Res. **4**, 023151 (2022).